

FREQUENCY SELECTIVE SHIELDING SCREEN BY THE USE OF ARTIFICIAL MEDIA

¹Tohru Iwai, ²Kennichi Hatakeyama

¹Sumitomo Electric Industries Inc., ²Faculty of Engineering, Himeji Institute of Technology
E-mail: ian-iwai@maia.conet.ne.jp

Abstract: We calculated the shielding characteristic of a three-dimensional array of strip conductors by using the electric field integral equation method and its expansion to an array structure. The reflection and transmission coefficients are calculated from the current distribution obtained, and the effective permittivity is calculated in wide frequency range. Above the resonant frequency, the effective permittivity becomes negative, and the transmission coefficient becomes very small because of the evanescent mode.

Key words: Electric field integral equation method, point matching method, effective permittivity, evanescent mode, shielding characteristic

1. Introduction

Artificial dielectrics were proposed more than 50 years ago. One type of artificial dielectrics comprises an array of conductors [1]. The conductors are polarized by an incident electric field in the same way as the atoms of an actual dielectric are polarized, and the array of conductors behaves macroscopically as an actual dielectric. The permittivity of an actual dielectric has frequency dispersion, and it is true for an

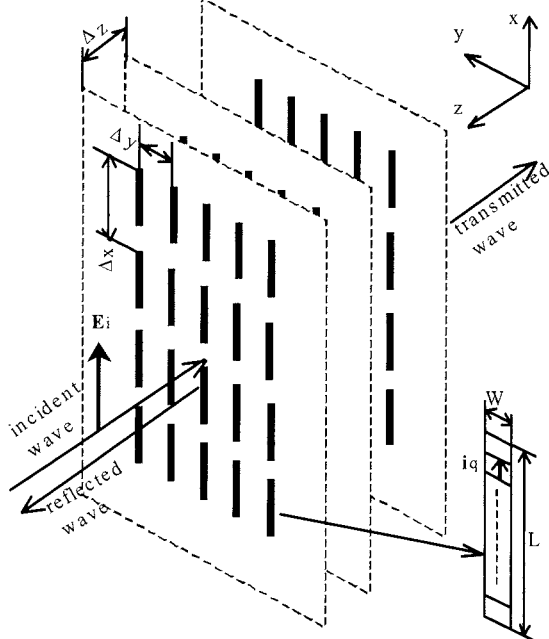


Fig.1 Three-dimensional array of strip conductors

artificial dielectric. A typical application of artificial dielectrics in the past was a lens antenna, but it was used in the frequency range much lower than the resonant frequency determined by the physical dimension of the conductor.

An application example of artificial dielectrics is an electromagnetic wave absorber, which consists of scattered metal fibers. It uses the resonance of the metal fibers and shows the dispersion of the permittivity [2] [3].

As another application of artificial dielectrics, we study frequency selective structure in this paper. A conventional frequency selective surface (FSS) comprises an array of conductors or slots, and it uses the resonance but it is treated as a ramped element circuit model [4]. We regard a three-dimensional array of strip conductors as an artificial dielectric showing the dispersion of its permittivity and shielding characteristic.

2. Simulation model and computational approach

2.1 Three-dimensional array of strip conductors

Fig.1 shows the three-dimensional array of strip conductors that we have simulated. The dimensions of each strip conductor are denoted by L in length and W in width. We assume the conductor is infinitely thin. The spacings of the conductor arrangement are Δx , Δy , and Δz for each direction. The numbers of strip conductors are infinite in both x - and y -direction, and N in z -direction. The incident waves are plane waves propagating from $+z$ toward $-z$ with electric fields parallel to x -axis.

2.2 Impedance matrix of the periodic conductors

A scattered electric field can be calculated from the current distribution by the use of the electric field integral equation method [5]. We start from considering a single conductor or a small number of conductors.

The scattered electric field is given by

$$\mathbf{E}_s(\mathbf{J}) = -j\omega\mathbf{A}(\mathbf{J}) - \nabla\phi(\mathbf{J}), \quad (1)$$

where $\mathbf{A}(\mathbf{J})$ is the electric vector potential and $\phi(\mathbf{J})$ is the electric scalar potential. The equation (1) can be expressed by an electric field integral equation:

$$\mathbf{E}_s = -j\omega\mu_0 \int_S \mathbf{J}(\mathbf{r}')G(\mathbf{r}, \mathbf{r}')ds' + \frac{1}{j\omega\epsilon_0} \nabla \int_S (\nabla' \cdot \mathbf{J}(\mathbf{r}'))G(\mathbf{r}, \mathbf{r}')ds', \quad (2)$$

where $G(\mathbf{r}, \mathbf{r}')$ is the free space Green's function:

$$G(\mathbf{r}, \mathbf{r}') = \frac{\exp(-jk|\mathbf{r} - \mathbf{r}'|)}{4\pi|\mathbf{r} - \mathbf{r}'|}, \quad (3)$$

where k is the wave number, \mathbf{r} is the vector of the observing point, and \mathbf{r}' is the vector of the source point. The total electric field at any point is the sum of the incident and scattered fields. On the conductor surface the tangential component of the electric field must be zero. So we obtain

$$\mathbf{n} \times \mathbf{E}_i = -\mathbf{n} \times \mathbf{E}_s \quad (\text{on } S), \quad (4)$$

where \mathbf{n} is a normal vector to the conductor surface.

We use the point matching method for the computation of the currents. Pulse functions and delta functions are used as basis functions and test functions. We obtain the system of linear equations (5), which determines the currents on the conductors.

$$\begin{pmatrix} z_{11} & \cdots & z_{1m} \\ \vdots & \ddots & \vdots \\ z_{m1} & \cdots & z_{mm} \end{pmatrix} \begin{pmatrix} i_1 \\ \vdots \\ i_m \end{pmatrix} = \begin{pmatrix} -E_{i1} \\ \vdots \\ -E_{im} \end{pmatrix}, \quad (5)$$

where i_q is the current densities of the q^{th} segment and E_{iq} is the incident electric field at the center of the segment. The impedance coefficients are given by

$$z_{pq} = -j\omega\mu_0 \int_S G(\mathbf{r}, \mathbf{r}')ds' + \frac{1}{j\omega\epsilon_0} \int_S (\nabla \cdot \mathbf{B}) \nabla_p G(\mathbf{r}, \mathbf{r}')ds', \quad (6)$$

where \mathbf{B}_q is the basis function of the q^{th} segment whose area is S_q and \mathbf{T}_p is the unit vector of the current direction of the p^{th} segment.

The next step is the expansion of this method to the analysis of the periodic array of conductors [6]. Some numbers of conductors are located in a unit cell. In this structure the conductors on the z -axis are in a unit cell and a great number of unit cells are allocated in x - y plane. Applying equation (5) into this structure, we obtain

$$\begin{pmatrix} z_{11}^{11} & \cdots & z_{1m}^{11} & \cdots & z_{11}^{11} & \cdots & z_{11}^{11} \\ \vdots & \ddots & \vdots & \ddots & \vdots & \ddots & \vdots \\ z_{m1}^{11} & \cdots & z_{mm}^{11} & \cdots & z_{m1}^{11} & \cdots & z_{mm}^{11} \\ \vdots & \ddots & \vdots & \ddots & \vdots & \ddots & \vdots \\ z_{11}^{11} & \cdots & z_{1m}^{11} & \cdots & z_{11}^{11} & \cdots & z_{1m}^{11} \\ \vdots & \ddots & \vdots & \ddots & \vdots & \ddots & \vdots \\ z_{m1}^{11} & \cdots & z_{mm}^{11} & \cdots & z_{m1}^{11} & \cdots & z_{mm}^{11} \end{pmatrix} \times \begin{pmatrix} i_1^1 \\ \vdots \\ i_m^1 \\ \vdots \\ i_1^w \\ \vdots \\ i_m^w \\ \vdots \\ i_1^w \\ \vdots \\ i_m^w \end{pmatrix} = \begin{pmatrix} -E_{i1}^1 \\ \vdots \\ -E_{im}^1 \\ \vdots \\ -E_{i1}^w \\ \vdots \\ -E_{im}^w \\ \vdots \\ -E_{i1}^w \\ \vdots \\ -E_{im}^w \end{pmatrix}, \quad (7)$$

where w is the number of unit cells, i_q^u is the q^{th} segment current of the u^{th} unit cell, E_{iq}^u is the inci-

dent electric field and z_{pq}^{uv} is the impedance coefficient between the q^{th} segment current of the v^{th} unit cell and the p^{th} segment current of the u^{th} unit cell.

Because all the unit cells are irradiated by the same incident electric field, they have the same current distribution. We obtain

$$E_{iq} = E_{iq}^1 = E_{iq}^2 = \cdots = E_{iq}^w \quad (q = 1, 2, \dots, m) \quad (8)$$

and

$$i_q = i_q^1 = i_q^2 = \cdots = i_q^w \quad (q = 1, 2, \dots, m). \quad (9)$$

The 1st row of (7) becomes

$$(z_{11}^{11} + z_{11}^{12} + \cdots)i_1 + (z_{12}^{11} + z_{12}^{12} + \cdots)i_2 + \cdots + (z_{1m}^{11} + z_{1m}^{12} + \cdots)i_m = -E_{i1}. \quad (10)$$

The general expression of (10) for infinite number of unit cells is

$$\sum_{q=1}^{\infty} \left(\sum_{v=1}^{\infty} z_{pq}^{1v} \right) i_q = -E_{ip} \quad (p = 1, 2, \dots, m). \quad (11)$$

We define new impedance coefficients as

$$z_{pq}^* = \sum_{v=1}^{\infty} z_{pq}^{1v}. \quad (12)$$

Using these impedance coefficients, we obtain

$$\begin{pmatrix} z_{11}^* & \cdots & z_{1m}^* \\ \vdots & \ddots & \vdots \\ z_{m1}^* & \cdots & z_{mm}^* \end{pmatrix} \begin{pmatrix} i_1 \\ \vdots \\ i_m \end{pmatrix} = \begin{pmatrix} -E_{i1} \\ \vdots \\ -E_{im} \end{pmatrix}. \quad (13)$$

The number of v in (12) in the calculation is discussed in 3.1.

3. Simulation Result

3.1 Calculation area and convergence of current

Calculations were carried out with the parameters shown in Table I. A strip conductor was divided into 20 segments (The size of each segment was 0.75mm by 0.75mm).

L:	length of a strip conductor	15 mm
W:	width of a strip conductor	0.75 mm
Δx :	spacing in x-direction	18 mm
Δy :	spacing in x-direction	3 mm
Δz :	spacing in z-direction	3 mm
N:	number of layers	5

In this simulation we calculated the conductors within a square area of x - y plane. The physical dimension of the calculation area is denoted by the factor of $\pm v_x$, a number of strip conductors taken into account for x -direction. As for v_y for y -direction, v_y is equal to $6v_x$.

Fig.2 shows the maximum currents induced on strip conductors versus v_x . The field strength of the incident wave is 1V/m.

As v_x increases, deviations of the maximum current decrease. Though the deviation depends on frequency, the deviations are less than 5% for v_x larger than 50, which is considered to be small enough to evaluate the strip-array effects.

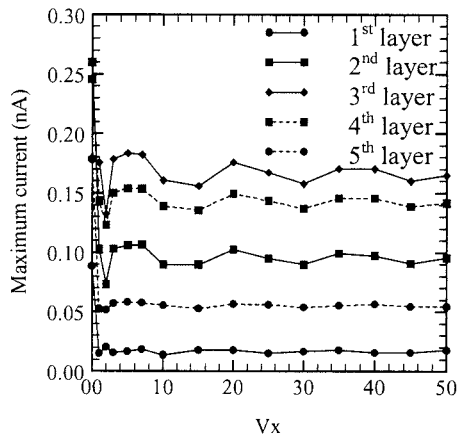


Fig.2 Maximum currents induced on the conductors versus v_x at $f=9\text{GHz}$. 1st layer means frontmost one of Fig.1

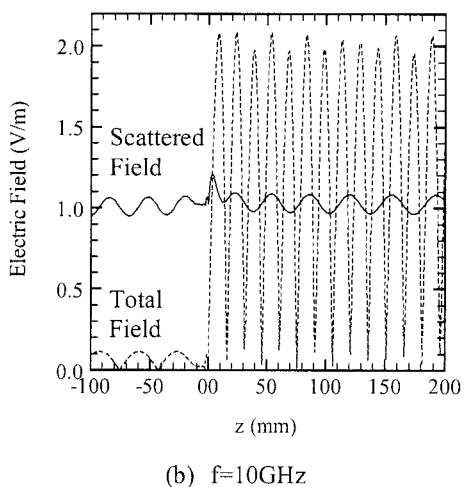
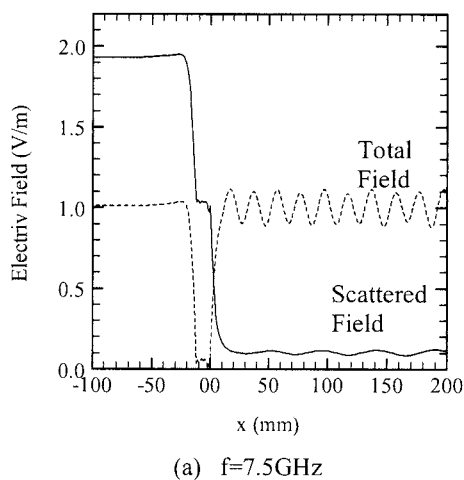


Fig.3 Scattered electric field and total electric field

3.2 Scattered and total electric field

Scattered electric fields are calculated using the currents on the strip conductors. Fig.3 shows the scattered electric fields and the total electric fields along z-axis at $f=7.5\text{GHz}$ and $f=10\text{GHz}$. In $z>0$ region the solid lines represent the reflected electric fields and the dotted lines show the standing-wave distributions. In $z<-12\text{mm}$ region the dotted lines represent the transmitted electric fields.

The fluctuations are observed in the scattered electric fields. At present, we think that phenomenon is caused by the calculation with the finite number of strip conductors.

As shown in Fig.3(a) and (b), the reflection is very small and almost all the incident waves are transmitted at $f=7.5\text{GHz}$, while the transmission is very small and almost all the incident waves are reflected at $f=10\text{GHz}$.

3.3 Reflection, transmission, and relative permittivity

The complex reflection and transmission coefficients for all frequency range can be calculated from the scattered and total electric fields. Figures 4 and 5

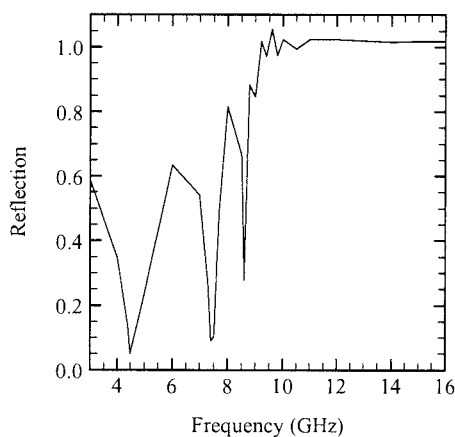


Fig.4 Reflection characteristic

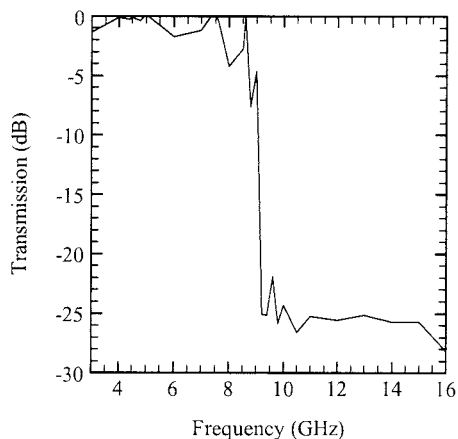


Fig.5 Transmission characteristic

show the frequency dependence of the amplitudes of the reflection and transmission coefficients. At the frequencies higher than 9GHz, almost all the incident waves are reflected, and the transmission becomes very small. At frequencies lower than 9GHz, the reflection coefficients are very small. From Fig.5 we find that the strip conductor array provides the excellent characteristics as a frequency selective shielding screen compared to the conventional FSS.

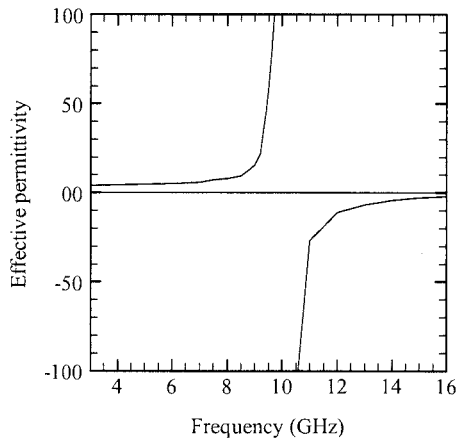


Fig.6 Effective Permittivity (real part)

When the array structure is considered as a homogeneous dielectric media, effective permittivity can be obtained by reflection or transmission coefficients.

The normalized input impedance Z_{in} is given as,

$$Z_{in} = \frac{1 + \frac{1}{\sqrt{\epsilon_r}} \tanh\left(j \frac{2\pi d}{\lambda_0} \sqrt{\epsilon_r}\right)}{1 + \sqrt{\epsilon_r} \tanh\left(j \frac{2\pi d}{\lambda_0} \sqrt{\epsilon_r}\right)} \quad (14)$$

where ϵ_r is the complex relative permittivity, d is the thickness, and λ is the wavelength in free space. We determined the boundaries of this array structure at $z=1.5\text{mm}$ and $z=-13.5\text{mm}$, so the thickness d is 15mm. Using the normalized input impedance calculated from the complex reflection coefficients, the complex relative permittivities are calculated numerically. Fig.6 shows the frequency characteristic of the real part of the effective permittivity: ϵ' . ϵ' is equal to 3.9 at $f=3\text{GHz}$. ϵ' increases as the frequency increases and diverges near the resonant frequency. At $f=9.9\text{GHz}$, ϵ' is less than -5000 and stays negative in the region $f \geq 9.9\text{GHz}$. In this frequency range, the polarization induced on a strip conductor is delayed in phase and it becomes in opposite direction to the incident electric field. An electromagnetic wave becomes an evanescent mode in a negative permittivity media in which the waves cannot propagate, so the transmission coefficient becomes very small.

The imaginary part is always around null within the calculation error. This means that this array structure is lossless, because we regard the strip conductors are perfect conductors.

At $f=4.5, 7.5, 8.6\text{GHz}$, the thickness of this array structure corresponds to 0.5, 1, and 1.5 times of the incident wavelength. So the reflected electric field from the back surface offsets that from the front surface. This phenomenon is actually observed in a real dielectric slab.

4. Conclusion

We simulated the dielectric characteristic of three-dimensional array of strip conductors using electric field integral equation method and its expansion to an array structure. The calculation results indicate that reflections and transmissions can be controlled by the array-structure factors such as the conductor length and the spacing of the arrangement. The effective permittivity of the array

- (1) increases as frequency increases below the resonant frequency,
- (2) diverges near the resonant frequency, and
- (3) becomes negative at frequencies higher than the resonant frequency.

It is clearly shown that the array-structure shows the negative effective permittivity that contributes to the frequency selective shielding characteristics. We are trying to design many devices using the artificial media.

References

- [1] W. E. Kock, "Metallic delay lenses," Bell Syst. Tech. J., Vol.27, pp58-82, Jan. 1948.
- [2] K. Hatakeyama and T. Inui, "Electromagnetic wave absorber using ferrite absorbing material dispersed with short metal fibers," IEEE Trans. Magnetism, Vol.MAG.-20, No.5, pp.1261-1263, Sep. 1984
- [3] T. Iwai, M. Yoshizawa, and H. Nakata, "Non-woven fabric type EM-wave absorber containing metal fibers," Technical Report of IEICE, EMCJ99-100, pp.67-72, Nov. 1999.
- [4] T. K. Wu, "Frequency selective surface and grid array," New York: John Wiley & Sons., 1995
- [5] M.F. Catedra, R.P. Torres, J. Basterrechea, and E. Gago, The CG-FFT Method, Norwood, MA: Artech House, 1995, Chap.5.
- [6] K. Hatakeyama and S. Hayashi, "Numerical approach for reflection and transmission of electromagnetic waves by finite length metal rods array," IEICE Trans. Commun., Vol.J81-B-II, No.10, pp.983-989, Oct. 1998